Coincident Multimessenger Bursts from Eccentric Supermassive Binary Black Holes

Vikram Manikantan[1*], Vasileios Paschalidis[1,2*] and Gabriele Bozzola[1,3]

[1]Steward Observatory & Department of Astronomy, University of Arizona, 933 N Cherry Avenue, Tucson, 85719, Arizona, USA.
[2]Department of Physics, University of Arizona, 1118 E. Fourth Street, Tucson, 85721, Arizona, USA.
[3]Division of Geological and Planetary Sciences, California Institute of Technology, 1200 E. California Blvd., Pasadena, 91125, California, USA.

*Corresponding author(s). E-mail(s): vik@arizona.edu; vpaschal@arizona.edu;

Abstract

Supermassive binary black holes are a key target for the future Laser Interferometer Space Antenna, and excellent multi-messenger sources with gravitational waves. However, unique features of their electromagnetic emission that are needed to distinguish them from single supermassive black holes are still being established. Here, we conduct the first magnetohydrodynamic simulation of accretion onto eccentric binary black holes in full general relativity incorporating synchrotron radiation transport through their dual-jet. We show that the total accretion rate, jet Poynting luminosity, and the optically thin synchrotron emission exhibit periodicity on the binary orbital period, demonstrating explicitly, for the first time, that the binary accretion rate periodicity can be reflected in its electromagnetic signatures. Additionally, we demonstrate that during each periodic cycle eccentric binaries spend more time in a *low* emission state than in a *high* state. Furthermore, we find that the gravitational wave bursts from eccentric binaries are coincident with the bursts in their jet luminosity and synchrotron emission. We discuss how multimessenger observations of these systems can probe plasma physics in their jet.

Keywords: Multi-messenger Astronomy, Black Holes, Gravitational Waves, Synchrotron Radiation

1 Introduction

The inspiral and merger of supermassive binary black holes (SMBBHs) are main targets for the future space-based gravitational wave (GW) Laser Interferometer Space Antenna (LISA) [1, 2]. At least a fraction of SMBBHs are expected to reside in hot, gaseous environments [3–5], making SMBBHs ideal for multimessenger astronomy because, in addition to GWs, their gas accretion will drive emission across the electromagnetic (EM) spectrum (see [6] for a recent review). Pulsar Timing Arrays (PTAs) also target SMBBHs, but unless their sensitivity increases significantly [7–9], detecting GWs from individual SMBBHs may have to wait until the launch of LISA in the mid 2030s.

Identifying EM signals that are unique to SMBBHs is essential to maximizing the scientific yield of multimessenger astronomy [10], and to probing fundamental physics, gravity, astrophysics, and cosmology with coincident EM and GW observations [1, 11, 12].

Over 200 SMBBH candidates have been identified through sky surveys [13–15], including more than 25 inferred to be in the strong-field dynamical regime [16]. Theoretical modeling of SMBBH accretion is crucial for predicting smoking-gun EM signatures of SMBBHs, and hence evaluating these potential relativistic candidates.

To reliably model SMBBH accretion from first principles during their late inspiral and merger requires simulations in full general relativity (GR) coupled to magnetohydrodynamics, microphysics and radiation. Performing such simulations with existing computational resources and numerical methods is not currently feasible due to the vast range of length and timescales involved. So, to make progress at this time, one has to make simplifying assumptions. Some methods forego relativistic gravity [17], and use 2D simulations (see, e.g., [18] and references therein for recent work). Others adopt post-Newtonian background metrics (see, e.g., [19] and references therein for recent work). Finally, fully general relativistic approaches solve the Einstein equations without approximation (see [20, 21] for reviews).

Recent studies of accretion onto binary black holes (BBH) in full $3+1$ GR have investigated various parameters [16, 22–26]. However, accretion onto eccentric SMBBHs in full GR remains unexplored. Treating eccentricity is essential, as an increasing number of works [27–30] show that disk-SMBBH interactions excite binary orbital eccentricity, with values reaching $e \simeq 0.3 - 0.5$ even in observable GW bands.

In this work, we present the first $3+1$ full GR magnetohydrodynamic simulation of circumbinary disk accretion onto a BBH with initial eccentricity $e = 0.3$, and perform the first synchrotron radiation transport calculation through the dual jet. We address two key questions: i) how does orbital eccentricity impact the mass accretion rate and its periodicity? ii) how does it affect the jet luminosity and synchrotron emission?

For a description of the methods and initial data we adopt in this work see Appendix A. Unless otherwise stated, we adopt geometrized units in which $G = c = 1$.

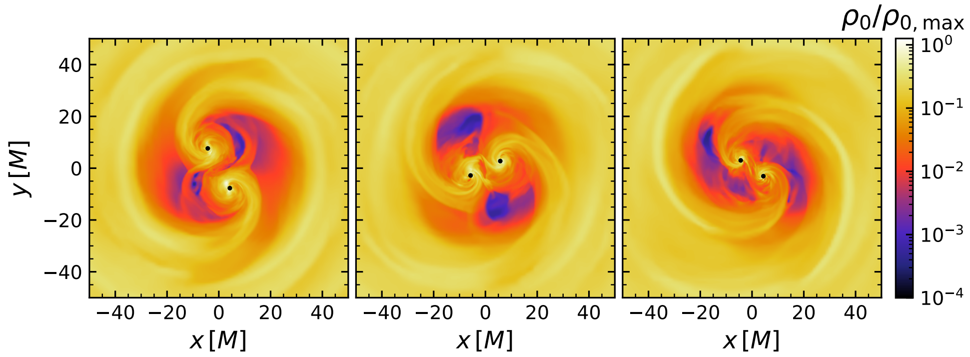

Fig. 1 Contours of rest-mass density (ρ_0) normalized to the initial maximum density $\rho_{0,\rm max} = 2.6 \times 10^{-11}(\dot{M}/0.1\dot{M}_{\rm edd})(M/10^7 M_\odot)^{-1}(\eta/0.1)^{-1}\,{\rm g\,cm^{-3}}$, where $\dot{M}$ is the accretion rate, $\dot{M}_{\rm edd}$ is the Eddington accretion rate for a gravitational mass M, and radiative efficiency η. The left panel corresponds to the binary just after apocenter ($t/M = 4120$), the center as it approaches pericenter ($t/M = 4220$), and the right at pericenter ($t/M = 4300$). We indicate the BH horizons with black disks. In the left panel, tidal streams circularize to form minidisks. In the center panel, these minidisks begin to accrete, and in the right panel are depleted at pericenter. Once in a quasi-steady-state, the binary exists in cavity with density $\rho_0/\rho_{0,\rm max} \sim 10^{-3} - 10^{-2}$.

2 Results

2.1 Accretion Flow

After initializing the torus around the BBH, we evolve the system until the accretion rate relaxes. In Fig. 1, we plot the rest-mass density of the gas on the BBH orbital plane at representative times: at pericenter (left), at apocenter (right), and an intermediate time (middle). We indicate the BH apparent horizons with black disks. The gas density is normalized to the initial maximum gas density in the torus, $\rho_{0,\rm max}$. The BHs continue to reside in a lower-density cavity ($\rho_0/\rho_{0,\rm max} \sim 10^{-3}$) within the higher-density circumbinary disk (CBD) ($\rho_0/\rho_{0,\rm max} \sim 1$). As the binary approaches the CBD inner edge at its apocenter, it tidally torques the CBD, and matter from the inner disk edge falls onto each BH through high-density tidal streams. The infalling gas temporarily circularizes around each BH creating a minidisk (left panel in Fig. 1), which begins to be depleted as the binary approaches the next pericenter passage (middle and right panels in Fig. 1). This process repeats quasi-periodically as the BBH inspirals.

In the left panel of Fig. 2, we plot the time-dependent total rest-mass accretion rate onto the BHs with a solid line, and the accretion rate onto the individual BHs with dashed lines. Both exhibit quasiperiodic behavior. In the right panel of Fig. 2, we plot the Fourier transform of the total rest-mass accretion rate for the time range $3000 < t/M < 5500$, which corresponds to about 5 binary orbits. The power spectral density (PSD) demonstrates that the dominant frequency of the accretion rate variability is the orbital frequency, $f \sim f_{\rm orb}$. This periodicity is consistent with recent Newtonian hydrodynamic studies of eccentric binaries (see [18] and references therein), which are valid for substantially larger orbital separations. The measured accretion rate

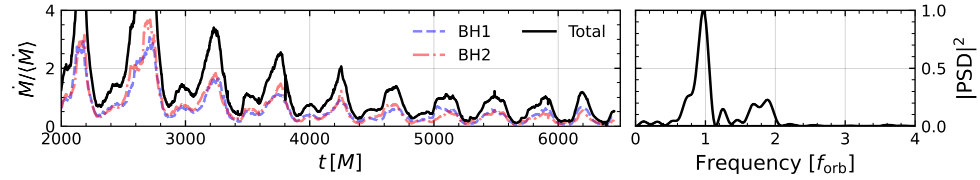

Fig. 2 Left: Rest-mass accretion rates onto both BHs (solid black line), and onto the individual black holes (dashed lines), all normalized by the total average for $3000 < t/M < 5500$. Right: Power spectral density (PSD) of the Fourier transform of the total rest-mass accretion rate, with the frequency normalized to the BBH orbital frequency. The Fourier transform is performed on the time period $t = 3000 - 5500\,M$. The dominant frequency for accretion is $f \sim f_{\rm orb}$, and is insensitive to time interval over which we perform the Fourier transform.

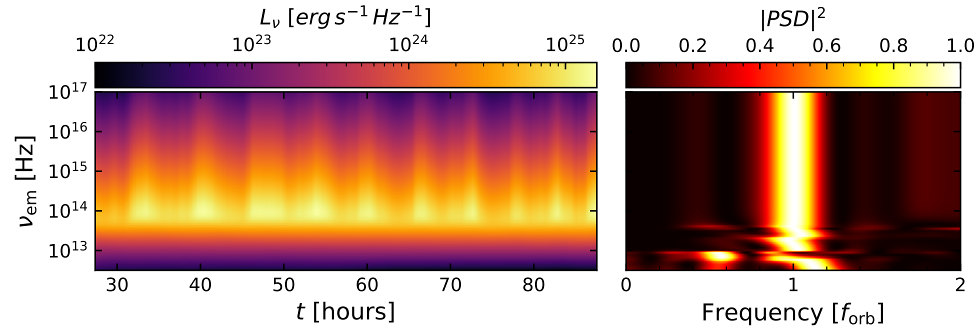

Fig. 3 Left: specific luminosity of synchrotron emission on a color scale vs time for a $10^7\,M_\odot$ binary accreting at 10% Eddington. The y-axis is the frequency of the SED and the x-axis the time, with the color bar indicating L_ν. Right: PSD of the Fourier transform of the frequency-binned SED time series. We perform the Fourier transform for the time period $t > 4000\,M$ ($t > 54.7$ hours). The plots demonstrate that only the optically thin region $\nu_{\rm em} \gtrsim 10^{14}$ Hz of the synchrotron SED has clear periodicity on the orbital timescale, of $f \sim f_{\rm orb}$, which matches its mass accretion rate periodicity and Poynting luminosity periodicity. There is no clear periodicity in the optically thick regime.

periodicity of $f_{\rm orb}$ in the eccentric case is fundamentally different from the periodicity in quasi-circular binaries, where the accretion rate is modulated at $1.4 f_{\rm orb}$ [16, 24]. We defer a detailed discussion of the dynamics and periodicity mechanisms in eccentric BBHs to a follow-up work where we explore more values of eccentricity [31].

2.2 Jet Synchrotron Emission

We observe dual jet launching along the BBH orbital angular momentum axis consistent with previous CBD studies in full GR with non-spinning black holes [16, 22–24]. Relativistic electrons within the jet's magnetic field can produce synchrotron emission across the EM spectrum (see, e.g., [32] for a review). In this section, we present spectral energy densities (SEDs) of the jet synchrotron emission by postprocessing our simulations. A detailed presentation of our synchrotron modeling, along with a derivation of analytic scalings of the SED with accretion rate and BBH mass, will be presented in a follow-up paper [31]. Here, we motivate our basic assumptions, and in Appendix A we discuss the relevant equations.

The interaction of the dual jets, which can give rise to current sheets and kink instabilities, can lead to a population of non-thermal electrons with power-law distribution [33–36]. Motivated by this, we make the following approximations in our synchrotron modeling: 1) we adopt a power-law electron distribution, assuming the local electron energy density equals 10% of the local magnetic energy density in the jet, i.e., we assume equipartition, which is fairly well established [34, 37–39]. However, we also tested a power-law distribution with minimum electron energy corresponding to a Lorentz factor of 2, as well as a thermal distribution [40, 41]; 2) We start our integrations at a height of $z/M = 50$ above the orbital plane. This is because we do not perform a general relativistic calculation, therefore our integration of the radiative transfer equation must be in approximately flat spacetime. However, we confirmed that the shape of the synchrotron spectrum and its variability are robust for integrations starting at $z/M = 20$ and $z/M = 30$; 3) We adopt the "fast light" approximation; we solve the radiative transfer equation on a slice of constant coordinate time. This approximation is valid when the medium does not change much on a light crossing time, which in our case is valid for the optically thin synchrotron frequencies; 4) We do not treat special relativistic effects other than those going into the computation of the synchrotron emissivity and absorption coefficient. This assumption is consistent with the fact that the plasma at the jet base in our simulations is only mildly relativistic ($v/c \sim 0.3$).

In this work we choose the power in the electron power-law distribution to be $p = 2.5$; In our follow-up extended paper [31] we will demonstrate that our reported results on the shape and the variability of the synchrotron spectrum are insensitive to p, and we will report the synchrotron spectra for quasicircular and other eccentric cases. Lastly, we only report results from a viewing angle of $\theta = 0$, in other words, we treat the system as a blazar. We solved the radiation transport equation for other viewing angles, and found that the shape and variability of the synchrotron spectrum are insensitive to the viewing angle, given the integration starts at the same height z. For the time-dependence of the synchrotron spectrum, we solve the radiative transfer equation with a cadence of $\sim 3.6\, GM/c^3$ and produce SEDs for each slice of constant coordinate time.

In the left panel of Fig. 3, we plot the SED vs time, assuming a $10^7\, M_\odot$ BBH accreting at 10% Eddington. The time-dependent SED is shown with a 2D color map where the y-axis indicates frequency and x-axis indicates increasing time in days, with the color indicating the specific luminosity. The frequency at peak synchrotron SED is $\nu_{\rm ssa} \sim 6 \times 10^{13}\,$Hz, where $\nu_{\rm ssa}$ is the synchrotron self-absorption frequency above (below) which the medium becomes optically thin (thick). This $\nu_{\rm ssa}$ is also a 'break' frequency, below which there is no clear variability. As the time evolution shows, the eccentric binary spends more time in a "low" state, where the synchrotron emission specific luminosity is minimum, followed by a sharp rise and decay in time, "high" state. Our calculations predict that a smoking-gun synchrotron signature of more eccentric binaries is that they spend longer time in the low state than in the high state. This is consistent with eccentric binaries spending more time at apocenter than pericenter.

We show the Fourier transforms of the binned-frequency synchrotron SED in the right panel of Fig. 3. The y-axis is the frequency of the EM spectrum, and the x-axis is the frequency (normalized by $f_{\rm orb}$) of the time variability of the specific luminosity within the frequency bin indicated on the y-axis. The color map shows the strength of the power spectral density. The plot demonstrates that the synchrotron SED exhibits variability at the orbital time $f \sim f_{\rm orb}$ in the optically thin regime (where $\nu_{\rm em} \gtrsim \nu_{\rm ssa}$) which is consistent with the variability of its rest-mass accretion rate (Figure 2). This is the first explicit demonstration that a jet EM signature periodicity matches the BBH accretion rate periodicity.

The synchrotron emission we report can be detected by NIRCam and MIRI on the James Webb Space Telescope [42], the upcoming Rubin Observatory and the Legacy Survey of Space and Time (LSST), as well as Roman Space Telescope [43]. The sensitivity of these instruments place limits on the distance of the detectability of the synchrotron signatures we predict. For example, we estimate that NIRCam could observe a $10^7 M_\odot$ BBH with $p = 2.5$ out to $\sim 1.4\,\text{Gpc}$, which corresponds to a redshift $z \sim 0.3$ assuming standard ΛCDM cosmology. We also repeated the calculation for a $10^9 M_\odot$ BBH, which is detectable out to $\sim 43\,\text{Gpc}$ ($z \sim 4.6$) [44]. All these distances are $\sim 10\times$ greater if we integrate for $z \geq 20\,M$. We estimated the ion temperature in the CBD and find temperatures of $\mathcal{O}(10^6\,\text{K})$. Therefore, the peak CBD thermal emission frequencies are $\mathcal{O}(10^{16}\,\text{Hz})$, consistent with previous work in full GR (see, e.g., [45]). Such frequencies are $O(100)\times$ larger than our reported peak synchrotron frequencies, rendering our predicted non-thermal spectrum more luminous and distinguishable from the CBD thermal spectrum near $\nu_{\rm ssa}$.

2.3 Coincident GW and EM Emission

In Fig. 4, we showcase the coincident GW and EM emission from our SMBBH. We plot the $\ell = 2, m = 2$ mode of the GW strain (top panel), the outgoing Poynting luminosity normalized by the time-averaged rest-mass accretion rate (middle panel), and the optically thin synchrotron luminosity (bottom panel) integrated for frequencies $\nu_{\rm em} \in [8 \times 10^{13} Hz, 8 \times 10^{14} Hz]$ (which sample the SED near the peak) all vs retarded time. The figure demonstrates that the GW and EM bursts happen almost simultaneously, as the GW bursts marginally precede the EM bursts in certain cases (see the second, third, and fourth peaks). A smoking-gun multimessenger signature of binaries with non-negligible eccentricity is that the time period between successive bursts is the same for both the GW and EM synchrotron emission.

3 Discussion

In this work, we presented the first simulation of magnetohydrodynamic disk accretion onto an equal-mass, non-spinning, eccentric binary black hole in $3+1$ full general relativity, incorporating synchrotron emission through the jet for the first time. Our key findings are: 1) The accretion rate onto eccentric BBHs in the strong-field dynamical spacetime is modulated with periodicity that matches the binary orbital frequency

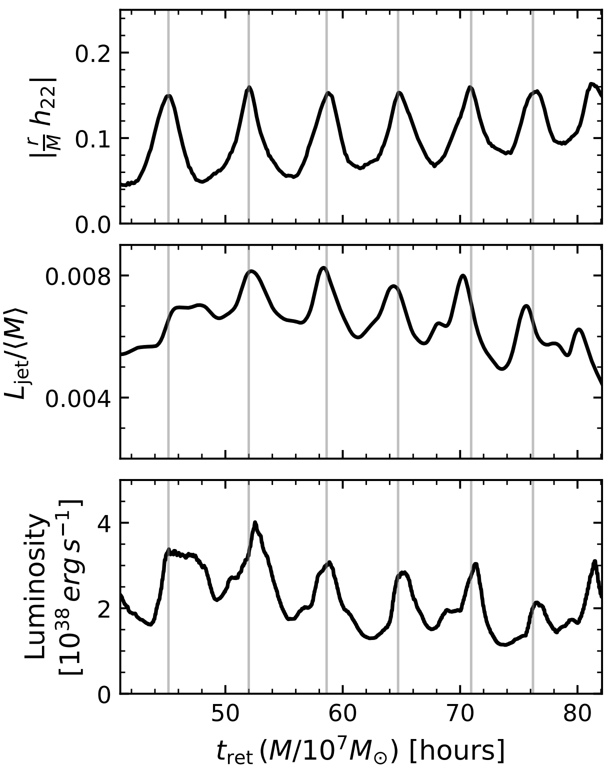

Fig. 4 Top row: Amplitude of the $\ell = 2, m = 2$ mode of the gravitational wave (GW) strain, $|h_{22}|$, normalized by the distance r/M vs retarded time $t_{\rm ret}$. Middle: Outgoing Poynting luminosity normalized by the rest-mass accretion rate vs $t_{\rm ret}$. Bottom: synchrotron luminosity integrated in the optically thin regime $8 \times 10^{13} Hz < \nu_{\rm em} < 8 \times 10^{14} Hz$ vs $t_{\rm ret}$ near peak emission. We denote the location of GW bursts with vertical translucent gray lines on both the GW and EM panels. The lightcurves shows almost perfect alignment between GW, Poynting flux, and EM bursts.

$f \sim f_{\rm orb}$, unlike quasicircular binaries for which this occurs at $f \sim 1.4 f_{\rm orb}$; 2) Eccentric binaries exhibit periodicity in the jet luminosity and optically thin synchrotron emission at the orbital frequency, $f_{\rm orb}$; A smoking-gun signature of eccentric binaries is that they spend more time in a low state (lower luminosity) than in a high state (higher luminosity) consistent with the time spent at apocenter and pericenter; 3) A smoking gun multimessenger signature of eccentric binaries is quasiperiodic bursts in their GWs, optically thin synchrotron emission, and jet luminosity, with identical delay times for consecutive EM and GW bursts.

We also experimented with different ways to set the energy density in the power-law distribution. If we do not assume equipartition between the electron and magnetic energy density, then variability is not as clear. Moreover, when we adopt a thermal distribution for the electrons the variability in the synchrotron SED also becomes unclear. This offers a unique opportunity to probe jet plasma physics with multi-messenger observations with GWs: LISA BBHs that are found to have substantial eccentricity ($O(0.1)$) can be followed up with EM observations to test jet variability. The existence, or lack, of variability of the synchrotron emission from the jet base in conjunction with theoretical modeling such as that performed in this work, can allow us to understand how electrons adapt to the changing magnetic field in a BBH spacetime. For example, lack of variability would inform us that either the electrons near the jet base are not in equipartition with the magnetic field or that they follow a thermal distribution. Regardless, the variability in the Poynting luminosity is robust, which implies that as the jet propagates into the interstellar and intergalactic medium it will generate emission in the radio that will exhibit variability on the binary orbital time, but at retarded time.

We conclude by listing some caveats: a fully general-relativistic ray-tracing and radiative transfer calculation is necessary to decipher the exact emission from the jet based all the way down to the BH horiozns, and to understand emission from the circumbinary disk, the inner cavity, and the minidisks. The latter is expected to be responsible for the bulk of the X-ray/UV emission as well as Doppler shifted emission lines [6]. Radiation feedback becomes important for accretion rates near the Eddington regime and must be accounted for. Therefore, our results are most applicable to sub-Eddington SMBBHs. Finally, it is important to consider a wide range of disk initial data and include spinning BHs. These will be the subject of future works of ours. However, the periodicities driven by eccentricity that we report here are robust. Hence, the qualitative features we have discovered in this work must be invariant under the aforementioned caveats.

Acknowledgements: this work was in part supported by NASA grant 80NSSC24K0771 and NSF grant PHY-2145421 to the University of Arizona. We thank Collin Christy for useful discussions. This research is part of the Frontera computing project at the Texas Advanced Computing Center. This research was in part supported by ACCESS under allocation award No. PHY190020. Frontera is made possible by National Science Foundation award OAC-1818253. ACCESS is supported by National Science Foundation grants 2138259, 2138286, 2138307, 2137603, and 2138296 [46].

A Methods

A.1 Initial data

Spacetime

We use the `TwoPunctures` thorn to generate the spacetime initial data for an equal-mass, non-spinning, eccentric BBH [47]. The BHs are initialized at apocenter with coordinate separation $d/M \simeq 26$. We introduce orbital eccentricity by first computing the 3rd-order Post-Newtonian linear momenta corresponding to a quasi-circular BBH, and then adjusting their tangential component by a factor of $\sqrt{1-e}$, where e is our target eccentricity.

Matter

We adopt the power-law torus solution for the matter initial conditions as previously described in [22, 23]. We set the inner edge of the circumbinary disk (CBD) at $r/M =$

18 with specific angular momentum of $l = 5.15$ and disk outer edge at $r/M \simeq 100$. We use a Γ-law equation of state, with $\Gamma = 4/3$ – appropriate for radiation dominated disks. We seed the disk with a poloidal magnetic field as in [23]. The initial magnetic field renders the CBD unstable to the magnetorotational instability (MRI) [48].

A.2 Evolution

Spacetime

We evolve the spacetime by solving full Einstein equations in the Baumgarte-Shapiro-Shibata-Nakamura (BSSN) formalism of general relativity [49, 50] as implemented in the `LeanBSSN` code using 6th-order finite differences [51]. We adopt the moving puncture gauge conditions [52, 53] with the shift vector parameter η set to $\eta = 1.4/M$.

Matter

We do not treat radiative feedback, heating, or cooling. Finally, the fluid does not backreact onto the spacetime, since the spacetime mass/energy content is dominated by the SMBBH. We employ the 3D general relativistic magnetohydrodynamic (GRMHD), adaptive-mesh-refinement (AMR) `IllinoisGRMHD` code [54] within the `Einstein Toolkit` [55], which employs the Cactus/Carpet infrastructure [56]. `IllinoisGRMHD` evolves the equations of ideal magnetohydrodynamics in flux-conservative form via the HLL Riemann solver [57], and the Piecewise-Parabolic reconstruction [58]. These methods have been described in [54] and have been extensively tested against other codes in [59]. For our EM gauge choice for the vector potential formulation of the induction equation, we use the generalized Lorenz gauge condition of [60] and set the Lorenz gauge damping parameter to $\xi = 8/M$.

Grid

We adopt `Carpet` [56] for adaptive mesh refinement (AMR). We use a three-dimensional Cartesian grid with the outer boundary extending from $-5120\,M$ to $+5120\,M$ in the x, y, and z directions, with a total of 14 refinement levels. We have 3 sets of nested AMR boxes, one centered on the center-of-mass, and two centered on each of the two BHs in the binary. The half side length of an AMR level i is $5120 \times 2^{-(i-1)}M$, $i = 1, \ldots 14$. The grid spacing on the coarsest (finest) refinement level is $\Delta x = 128\,M$ ($\Delta x = M/64$). Our grid resolves the fastest growing mode MRI wavelength with at least 20 zones in the disk and a maximum of 50 zones at the inner edge of the disk.

Diagnostics

We adopt the same diagnostic tools as in [24], to measure the rest-mass accretion rate ($\dot{M}$), and outgoing Poynting flux. The latter we compute on a sphere of coordinate radius $200\,M$ from the binary center of mass, thereby encompassing the entire BBH-disk system. We locate apparent horizons with `AHFinderDirect` [61]. We perform all Fourier analysis with the `scipy.fft` function [62]. We measure the orbital frequency of the binary with the Fourier transform of the first time derivative of the unfolded phase (φ) of the $\ell, m = (2, 2)$ mode, $f_{22} \equiv \frac{d\varphi}{dt}$, which we extract using the `NPScalars` thorn part of Canuda suite [63]. We use the package `kuibit` [64] for all our analysis.

A.3 Synchrotron modeling

To model synchrotron emission, we solve the radiation transfer equation (1.23) of [40], using the synchrotron emissivity given by Eq. (6.36) of [40] multiplied by $1/4\pi$, i.e., we average out the distribution over solid angle. Moreover, in the emissivity we average the pitch angle, α, out of the equation by assuming that the electrons follow an isotropic pitch angle distribution between $0 < \alpha < \pi/2$. We adopt the synchrotron self-absorption coefficient given by Eq. (6.53) of [40]. This emissivity and absorption coefficient corresponds to a power-law electron distribution $N(E)\,dE = CE^{-p}\,dE$. This distribution has two constants that define it for a given p: C and the miminum electron energy $E_{\min}$. To compute C, we impose charge neutrality with the ion density in our simulations, and compute E_1 either by adopting equipartition between the electrons and the magnetic fields – energy density of electrons equals 10% of the magnetic energy density – or we set $E_1 = 2m_e c^2$, where m_e is the electron mass. For thermal synchrotron we follow [40, 41].

References

[1] Consortium, T., Seoane, P.A., Aoudia, S., Audley, H., Auger, G., Babak, S., Baker, J., Barausse, E., Barke, S., Bassan, M., Beckmann, V., Benacquista, M., Bender, P.L., Berti, E., Binétruy, P., Bogenstahl, J., Bonvin, C., Bortoluzzi, D., Brause, N.C., Brossard, J., Buchman, S., Bykov, I., Camp, J., Caprini, C., Cavalleri, A., Cerdonio, M., Ciani, G., Colpi, M., Congedo, G., Conklin, J., Cornish, N., Danzmann, K., Vine, G., DeBra, D., Freitag, M.D., Di Fiore, L., Aguilo, M.D., Diepholz, I., Dolesi, R., Dotti, M., Barranco, G.F., Ferraioli, L., Ferroni, V., Finetti, N., Fitzsimons, E., Gair, J., Galeazzi, F., Garcia, A., Gerberding, O., Gesa, L., Giardini, D., Gibert, F., Grimani, C., Groot, P., Cervantes, F.G., Haiman, Z., Halloin, H., Heinzel, G., Hewitson, M., Hogan, C., Holz, D., Hornstrup, A., Hoyland, D., Hoyle, C.D., Hueller, M., Hughes, S., Jetzer, P., Kalogera, V., Karnesis, N., Kilic, M., Killow, C., Klipstein, W., Kochkina, E., Korsakova, N., Krolak, A., Larson, S., Lieser, M., Littenberg, T., Livas, J., Lloro, I., Mance, D., Madau, P., Maghami, P., Mahrdt, C., Marsh, T., Mateos, I., Mayer, L., McClelland, D., McKenzie, K., McWilliams, S., Merkowitz, S., Miller, C., Mitryk, S., Moerschell, J., Mohanty, S., Monsky, A., Mueller, G., Müller, V., Nelemans, G., Nicolodi, D., Nissanke, S., Nofrarias, M., Numata, K., Ohme, F., Otto, M., Perreur-Lloyd, M., Petiteau, A., Phinney, E.S., Plagnol, E., Pollack, S., Porter, E., Prat, P., Preston, A., Prince, T., Reiche, J., Richstone, D., Robertson, D., Rossi, E.M., Rosswog, S., Rubbo, L., Ruiter, A., Sanjuan, J., Sathyaprakash, B.S., Schlamminger, S., Schutz, B., Schütze, D., Sesana, A., Shaddock, D., Shah, S., Sheard, B., Sopuerta, C.F., Spector, A., Spero, R., Stanga, R., Stebbins, R., Stede, G., Steier, F., Sumner, T., Sun, K.-X., Sutton, A., Tanaka, T., Tanner, D., Thorpe, I., Tröbs, M., Tinto, M., Tu, H.-B., Vallisneri, M., Vetrugno, D., Vitale, S., Volonteri, M., Wand, V., Wang, Y., Wanner, G., Ward, H., Ware, B., Wass, P.,

Weber, W.J., Yu, Y., Yunes, N., Zweifel, P.: The Gravitational Universe (2013). arXiv:1305.5720 [astro-ph, physics:gr-qc]. Accessed 2023-09-12

[2] LISA Consortium Waveform Working Group, Afshordi, N., Akçay, S., Amaro Seoane, P., Antonelli, A., Aurrekoetxea, J.C., Barack, L., Barausse, E., Benkel, R., Bernard, L., Bernuzzi, S., Berti, E., Bonetti, M., Bonga, B., Bozzola, G., Brito, R., Buonanno, A., Cárdenas-Avendaño, A., Casals, M., Chernoff, D.F., Chua, A.J.K., Clough, K., Colleoni, M., Dhesi, M., Druart, A., Durkan, L., Faye, G., Ferguson, D., Field, S.E., Gabella, W.E., García-Bellido, J., Gracia-Linares, M., Gerosa, D., Green, S.R., Haney, M., Hannam, M., Heffernan, A., Hinderer, T., Helfer, T., Hughes, S.A., Husa, S., Isoyama, S., Katz, M.L., Kavanagh, C., Khanna, G., Kidder, L.E., Korol, V., Küchler, L., Laguna, P., Larrouturou, F., Le Tiec, A., Leather, B., Lim, E.A., Lim, H., Littenberg, T.B., Long, O., Lousto, C.O., Lovelace, G., Lukes-Gerakopoulos, G., Lynch, P., Macedo, R.P., Markakis, C., Maggio, E., Mandel, I., Maselli, A., Mathews, J., Mourier, P., Neilsen, D., Nagar, A., Nichols, D.A., Novák, J., Okounkova, M., O'Shaughnessy, R., Oshita, N., O'Toole, C., Pan, Z., Pani, P., Pappas, G., Paschalidis, V., Pfeiffer, H.P., Pompili, L., Pound, A., Pratten, G., Rüter, H.R., Ruiz, M., Sam, Z., Sberna, L., Shapiro, S.L., Shoemaker, D.M., Sopuerta, C.F., Spiers, A., Sundar, H., Tamanini, N., Thompson, J.E., Toubiana, A., Tsokaros, A., Upton, S.D., Meent, M., Vernieri, D., Wachter, J.M., Warburton, N., Wardell, B., Witek, H., Witzany, V., Yang, H., Zilhão, M., Albertini, A., Arun, K.G., Bezares, M., Bonilla, A., Chapman-Bird, C., Cownden, B., Cunningham, K., Devitt, C., Dolan, S., Duque, F., Dyson, C., Fryer, C.L., Gair, J.R., Giacomazzo, B., Gupta, P., Han, W.-B., Haas, R., Hirschmann, E.W., Huerta, E.A., Jetzer, P., Kelly, B., Khalil, M., Lewis, J., Lloyd-Ronning, N., Marsat, S., Nardini, G., Neef, J., Ottewill, A., Pantelidou, C., Piovano, G.A., Redondo-Yuste, J., Sagunski, L., Stein, L.C., Skoupý, V., Sperhake, U., Speri, L., Spieksma, T.F.M., Stevens, C., Trestini, D., Vañó-Viñuales, A.: Waveform Modelling for the Laser Interferometer Space Antenna. Publication Title: arXiv e-prints ADS Bibcode: 2023arXiv231101300L (2023). https://doi.org/10.48550/arXiv.2311.01300 . https://ui.adsabs.harvard.edu/abs/2023arXiv231101300L Accessed 2024-09-13

[3] Rodriguez, C., Taylor, G.B., Zavala, R.T., Pihlström, Y.M., Peck, A.B.: H I Observations of the Supermassive Binary Black Hole System in 0402+379. The Astrophysical Journal **697**, 37–44 (2009) https://doi.org/10.1088/0004-637X/697/1/37 . ADS Bibcode: 2009ApJ...697...37R. Accessed 2023-09-12

[4] Ivanova, N., Chaichenets, S., Fregeau, J., Heinke, C.O., Lombardi, J.C. Jr., Woods, T.E.: Formation of Black Hole X-ray Binaries in Globular Clusters. The Astrophysical Journal **717**, 948–957 (2010) https://doi.org/10.1088/0004-637X/717/2/948 . ADS Bibcode: 2010ApJ...717..948I. Accessed 2024-01-31

[5] Li, S., Berczik, P., Chen, X., Liu, F.K., Spurzem, R., Qiu, Y.: Direct N-body Simulations of Tidal Disruption Rate Evolution in Unequal-mass Galaxy Mergers. The Astrophysical Journal **883**, 132 (2019) https://doi.org/10.3847/1538-4357/

ab3e4a . ADS Bibcode: 2019ApJ...883..132L. Accessed 2024-01-31

[6] Bogdanovic, T., Miller, M.C., Blecha, L.: Electromagnetic Counterparts to Massive Black Hole Mergers. Living Reviews in Relativity **25**(1), 3 (2022) https://doi.org/10.1007/s41114-022-00037-8 . arXiv:2109.03262 [astro-ph, physics:gr-qc]. Accessed 2022-11-10

[7] Afzal, A., Agazie, G., Anumarlapudi, A., Archibald, A.M., Arzoumanian, Z., Baker, P.T., Bécsy, B., Blanco-Pillado, J.J., Blecha, L., Boddy, K.K., Brazier, A., Brook, P.R., Burke-Spolaor, S., Burnette, R., Case, R., Charisi, M., Chatterjee, S., Chatziioannou, K., Cheeseboro, B.D., Chen, S., Cohen, T., Cordes, J.M., Cornish, N.J., Crawford, F., Cromartie, H.T., Crowter, K., Cutler, C.J., DeCesar, M.E., DeGan, D., Demorest, P.B., Deng, H., Dolch, T., Drachler, B., Eckardstein, R.v., Ferrara, E.C., Fiore, W., Fonseca, E., Freedman, G.E., Garver-Daniels, N., Gentile, P.A., Gersbach, K.A., Glaser, J., Good, D.C., Guertin, L., Gültekin, K., Hazboun, J.S., Hourihane, S., Islo, K., Jennings, R.J., Johnson, A.D., Jones, M.L., Kaiser, A.R., Kaplan, D.L., Kelley, L.Z., Kerr, M., Key, J.S., Laal, N., Lam, M.T., Lamb, W.G., Lazio, T.J.W., Lee, V.S.H., Lewandowska, N., Santos, R.R.L.d., Littenberg, T.B., Liu, T., Lorimer, D.R., Luo, J., Lynch, R.S., Ma, C.-P., Madison, D.R., McEwen, A., McKee, J.W., McLaughlin, M.A., McMann, N., Meyers, B.W., Meyers, P.M., Mingarelli, C.M.F., Mitridate, A., Nay, J., Natarajan, P., Ng, C., Nice, D.J., Ocker, S.K., Olum, K.D., Pennucci, T.T., Perera, B.B.P., Petrov, P., Pol, N.S., Radovan, H.A., Ransom, S.M., Ray, P.S., Romano, J.D., Sardesai, S.C., Schmiedekamp, A., Schmiedekamp, C., Schmitz, K., Schröder, T., Schult, L., Shapiro-Albert, B.J., Siemens, X., Simon, J., Siwek, M.S., Stairs, I.H., Stinebring, D.R., Stovall, K., Stratmann, P., Sun, J.P., Susobhanan, A., Swiggum, J.K., Taylor, J., Taylor, S.R., Trickle, T., Turner, J.E., Unal, C., Vallisneri, M., Verma, S., Vigeland, S.J., Wahl, H.M., Wang, Q., Witt, C.A., Wright, D., Young, O., Zurek, K.M., Collaboration, T.N.: The NANOGrav 15 yr Data Set: Search for Signals from New Physics. The Astrophysical Journal Letters **951**(1), 11 (2023) https://doi.org/10.3847/2041-8213/acdc91 . Publisher: The American Astronomical Society. Accessed 2023-09-28

[8] Kelley, L.Z., Blecha, L., Hernquist, L., Sesana, A., Taylor, S.R.: Single sources in the low-frequency gravitational wave sky: properties and time to detection by pulsar timing arrays. Monthly Notices of the Royal Astronomical Society **477**, 964–976 (2018) https://doi.org/10.1093/mnras/sty689 . Publisher: OUP ADS Bibcode: 2018MNRAS.477..964K. Accessed 2024-09-16

[9] Babak, S., Falxa, M., Franciolini, G., Pieroni, M.: Forecasting the sensitivity of pulsar timing arrays to gravitational wave backgrounds. Physical Review D **110**(6), 063022 (2024) https://doi.org/10.1103/PhysRevD.110.063022 . Publisher: American Physical Society. Accessed 2024-09-20

[10] Schnittman, J.D.: Electromagnetic counterparts to black hole mergers. Classical and Quantum Gravity **28**(9), 094021 (2011) https://doi.org/10.1088/0264-9381/

28/9/094021

[11] Arun, K.G., Belgacem, E., Benkel, R., Bernard, L., Berti, E., Bertone, G., Besancon, M., Blas, D., Böhmer, C.G., Brito, R., Calcagni, G., Cardenas-Avendaño, A., Clough, K., Crisostomi, M., De Luca, V., Doneva, D., Escoffier, S., Ezquiaga, J.M., Ferreira, P.G., Fleury, P., Foffa, S., Franciolini, G., Frusciante, N., García-Bellido, J., Herdeiro, C., Hertog, T., Hinderer, T., Jetzer, P., Lombriser, L., Maggio, E., Maggiore, M., Mancarella, M., Maselli, A., Nampalliwar, S., Nichols, D., Okounkova, M., Pani, P., Paschalidis, V., Raccanelli, A., Randall, L., Renaux-Petel, S., Riotto, A., Ruiz, M., Saffer, A., Sakellariadou, M., Saltas, I.D., Sathyaprakash, B.S., Shao, L., Sopuerta, C.F., Sotiriou, T.P., Stergioulas, N., Tamanini, N., Vernizzi, F., Witek, H., Wu, K., Yagi, K., Yazadjiev, S., Yunes, N., Zilhão, M., Afshordi, N., Angonin, M.-C., Baibhav, V., Barausse, E., Barreiro, T., Bartolo, N., Bellomo, N., Ben-Dayan, I., Bergshoeff, E.A., Bernuzzi, S., Bertacca, D., Bhagwat, S., Bonga, B., Burko, L.M., Compére, G., Cusin, G., Silva, A., Das, S., Rham, C., Destounis, K., Dimastrogiovanni, E., Duque, F., Easther, R., Farmer, H., Fasiello, M., Fisenko, S., Fransen, K., Frauendiener, J., Gair, J., Gergely, L.A., Gerosa, D., Gualtieri, L., Han, W.-B., Hees, A., Helfer, T., Hennig, J., Jenkins, A.C., Kajfasz, E., Kaloper, N., Karas, V., Kavanagh, B.J., Klioner, S.A., Koushiappas, S.M., Lagos, M., Poncin-Lafitte, C.L., Lobo, F.S.N., Markakis, C., Martín-Moruno, P., Martins, C.J.A.P., Matarrese, S., Mayerson, D.R., Mimoso, J.P., Noller, J., Nunes, N.J., Oliveri, R., Orlando, G., Pappas, G., Pikovski, I., Pilo, L., Podolský, J., Pratten, G., Prokopec, T., Qi, H., Rastgoo, S., Ricciardone, A., Rollo, R., Rubiera-Garcia, D., Sergijenko, O., Shapiro, S., Shoemaker, D., Spallicci, A., Stashko, O., Stein, L.C., Tasinato, G., Tolley, A.J., Vagenas, E.C., Vandoren, S., Vernieri, D., Vicente, R., Wiseman, T., Zhdanov, V.I., Zumalacárregui, M.: New horizons for fundamental physics with LISA. Living Reviews in Relativity **25**, 4 (2022) https://doi.org/10.1007/s41114-022-00036-9 . ADS Bibcode: 2022LRR....25....4A. Accessed 2024-09-13

[12] Amaro-Seoane, P., Andrews, J., Arca Sedda, M., Askar, A., Baghi, Q., Balasov, R., Bartos, I., Bavera, S.S., Bellovary, J., Berry, C.P.L., Berti, E., Bianchi, S., Blecha, L., Blondin, S., Bogdanović, T., Boissier, S., Bonetti, M., Bonoli, S., Bortolas, E., Breivik, K., Capelo, P.R., Caramete, L., Cattorini, F., Charisi, M., Chaty, S., Chen, X., Chruślińska, M., Chua, A.J.K., Church, R., Colpi, M., D'Orazio, D., Danielski, C., Davies, M.B., Dayal, P., De Rosa, A., Derdzinski, A., Destounis, K., Dotti, M., Dutan, I., Dvorkin, I., Fabj, G., Foglizzo, T., Ford, S., Fouvry, J.-B., Franchini, A., Fragos, T., Fryer, C., Gaspari, M., Gerosa, D., Graziani, L., Groot, P., Habouzit, M., Haggard, D., Haiman, Z., Han, W.-B., Istrate, A., Johansson, P.H., Khan, F.M., Kimpson, T., Kokkotas, K., Kong, A., Korol, V., Kremer, K., Kupfer, T., Lamberts, A., Larson, S., Lau, M., Liu, D., Lloyd-Ronning, N., Lodato, G., Lupi, A., Ma, C.-P., Maccarone, T., Mandel, I., Mangiagli, A., Mapelli, M., Mathis, S., Mayer, L., McGee, S., McKernan, B., Miller, M.C., Mota, D.F., Mumpower, M., Nasim, S.S., Nelemans, G., Noble, S., Pacucci, F., Panessa, F., Paschalidis, V., Pfister, H., Porquet, D., Quenby, J., Ricarte, A., Röpke, F.K., Regan, J., Rosswog, S., Ruiter, A., Ruiz, M., Runnoe,

J., Schneider, R., Schnittman, J., Secunda, A., Sesana, A., Seto, N., Shao, L., Shapiro, S., Sopuerta, C., Stone, N.C., Suvorov, A., Tamanini, N., Tamfal, T., Tauris, T., Temmink, K., Tomsick, J., Toonen, S., Torres-Orjuela, A., Toscani, M., Tsokaros, A., Unal, C., Vázquez-Aceves, V., Valiante, R., Putten, M., Roestel, J., Vignali, C., Volonteri, M., Wu, K., Younsi, Z., Yu, S., Zane, S., Zwick, L., Antonini, F., Baibhav, V., Barausse, E., Bonilla Rivera, A., Branchesi, M., Branduardi-Raymont, G., Burdge, K., Chakraborty, S., Cuadra, J., Dage, K., Davis, B., Mink, S.E., Decarli, R., Doneva, D., Escoffier, S., Gandhi, P., Haardt, F., Lousto, C.O., Nissanke, S., Nordhaus, J., O'Shaughnessy, R., Portegies Zwart, S., Pound, A., Schussler, F., Sergijenko, O., Spallicci, A., Vernieri, D., Vigna-Gómez, A.: Astrophysics with the Laser Interferometer Space Antenna. Living Reviews in Relativity **26**, 2 (2023) https://doi.org/10.1007/s41114-022-00041-y . ADS Bibcode: 2023LRR....26....2A. Accessed 2024-09-12

[13] Charisi, M., Bartos, I., Haiman, Z., Price-Whelan, A.M., Márka, S.: Multiple periods in the variability of the supermassive black hole binary candidate quasar PG1302-102? Monthly Notices of the Royal Astronomical Society **454**, 21–25 (2015) https://doi.org/10.1093/mnrasl/slv111 . ADS Bibcode: 2015MNRAS.454L..21C. Accessed 2024-02-12

[14] Graham, M.J., Djorgovski, S.G., Stern, D., Drake, A.J., Mahabal, A.A., Donalek, C., Glikman, E., Larson, S., Christensen, E.: A systematic search for close supermassive black hole binaries in the Catalina Real-time Transient Survey. Monthly Notices of the Royal Astronomical Society **453**(2), 1562–1576 (2015) https://doi.org/10.1093/mnras/stv1726 . Accessed 2024-02-12

[15] Liu, T., Gezari, S., Ayers, M., Burgett, W., Chambers, K., Hodapp, K., Huber, M.E., Kudritzki, R.-P., Metcalfe, N., Tonry, J., Wainscoat, R., Waters, C.: Supermassive Black Hole Binary Candidates from the Pan-STARRS1 Medium Deep Survey. The Astrophysical Journal **884**(1), 36 (2019) https://doi.org/10.3847/1538-4357/ab40cb . Publisher: The American Astronomical Society. Accessed 2023-09-13

[16] Paschalidis, V., Bright, J., Ruiz, M., Gold, R.: Minidisk dynamics in accreting, spinning black hole binaries: Simulations in full general relativity. The Astrophysical Journal Letters **910**(2), 26 (2021) https://doi.org/10.3847/2041-8213/abee21 . arXiv:2102.06712 [astro-ph, physics:gr-qc]. Accessed 2023-03-21

[17] Most, E.R., Wang, H.-Y.: Decoupling of a supermassive black hole binary from its magnetically arrested circumbinary accretion disk (2024) arXiv:2410.23264 [astro-ph.HE]

[18] DeLaurentiis, S., Haiman, Z., Westernacher-Schneider, J.R., Krauth, L.M., Davelaar, J., Zrake, J., MacFadyen, A.: Relativistic Binary Precession: Impact on Eccentric Binary Accretion and Multi-Messenger Astronomy. arXiv. arXiv:2405.07897 [astro-ph] (2024). http://arxiv.org/abs/2405.07897 Accessed 2024-05-21

[19] Avara, M.J., Krolik, J.H., Campanelli, M., Noble, S.C., Bowen, D., Ryu, T.: Accretion onto a Supermassive Black Hole Binary Before Merger. arXiv. arXiv:2305.18538 [astro-ph, physics:gr-qc] (2023). http://arxiv.org/abs/2305.18538 Accessed 2023-08-21

[20] Gold, R.: Relativistic Aspects of Accreting Supermassive Black Hole Binaries in Their Natural Habitat: A Review. Galaxies **7**(2), 63 (2019) https://doi.org/10.3390/galaxies7020063 . Accessed 2022-11-10

[21] Cattorini, F., Giacomazzo, B.: GRMHD study of accreting massive black hole binaries in astrophysical environment: A review. Astropart. Phys. **154**, 102892 (2024) https://doi.org/10.1016/j.astropartphys.2023.102892 arXiv:2401.02521 [astro-ph.HE]

[22] Gold, R., Paschalidis, V., Ruiz, M., Shapiro, S.L., Etienne, Z.B., Pfeiffer, H.P.: Accretion disks around binary black holes of unequal mass: General relativistic MHD simulations of postdecoupling and merger. Physical Review D **90**(10), 104030 (2014) https://doi.org/10.1103/PhysRevD.90.104030 . Accessed 2023-03-21

[23] Khan, A., Paschalidis, V., Ruiz, M., Shapiro, S.L.: Disks Around Merging Binary Black Holes: From GW150914 to Supermassive Black Holes. Physical Review D **97**(4), 044036 (2018) https://doi.org/10.1103/PhysRevD.97.044036 . arXiv:1801.02624 [astro-ph, physics:gr-qc]. Accessed 2024-03-20

[24] Bright, J.C., Paschalidis, V.: Minidisk Influence on Flow Variability in Accreting Spinning Black Hole Binaries: Simulations in Full General Relativity. Monthly Notices of the Royal Astronomical Society **520**(1), 392–401 (2023) https://doi.org/10.1093/mnras/stad091 . arXiv:2210.15686 [astro-ph, physics:gr-qc]. Accessed 2023-09-08

[25] Cattorini, F., Maggioni, S., Giacomazzo, B., Haardt, F., Colpi, M., Covino, S.: Misaligned Spinning Binary Black Hole Mergers in Hot Magnetized Plasma. The Astrophysical Journal Letters **930**(1), 1 (2022) https://doi.org/10.3847/2041-8213/ac6755 . arXiv:2202.08282 [astro-ph, physics:gr-qc]. Accessed 2024-08-22

[26] Ruiz, M., Tsokaros, A., Shapiro, S.L.: General Relativistic Magnetohydrodynamic Simulations of Accretion Disks Around Tilted Binary Black Holes of Unequal Mass. arXiv. arXiv:2302.09083 [astro-ph, physics:gr-qc] (2023). https://doi.org/10.48550/arXiv.2302.09083 . http://arxiv.org/abs/2302.09083 Accessed 2024-08-22

[27] Roedig, C., Dotti, M., Sesana, A., Cuadra, J., Colpi, M.: Limiting eccentricity of subparsec massive black hole binaries surrounded by self-gravitating gas discs. Monthly Notices of the Royal Astronomical Society **415**, 3033–3041 (2011) https://doi.org/10.1111/j.1365-2966.2011.18927.x . Publisher: OUP ADS

Bibcode: 2011MNRAS.415.3033R. Accessed 2024-09-27

[28] Siwek, M., Kelley, L.Z., Hernquist, L.: Signatures of Circumbinary Disk Dynamics in Multi-Messenger Population Studies of Massive Black Hole Binaries. arXiv. arXiv:2403.08871 [astro-ph] (2024). http://arxiv.org/abs/2403.08871 Accessed 2024-03-28

[29] Valli, R., Tiede, C., Vigna-Gómez, A., Cuadra, J., Siwek, M., Ma, J.-Z., D'Orazio, D.J., Zrake, J., Mink, S.E.: Long-term Evolution of Binary Orbits Induced by Circumbinary Disks. arXiv. arXiv:2401.17355 [astro-ph] (2024). http://arxiv.org/abs/2401.17355 Accessed 2024-02-01

[30] Franchini, A., Prato, A., Longarini, C., Sesana, A.: On the behaviour of eccentric sub-pc massive black hole binaries embedded in massive discs. Publication Title: arXiv e-prints ADS Bibcode: 2024arXiv240200938F (2024). https://doi.org/10.48550/arXiv.2402.00938 . https://ui.adsabs.harvard.edu/abs/2024arXiv240200938F Accessed 2024-02-13

[31] Manikantan, V., Paschalidis, V., Bozzola, G. In preparation (2024)

[32] Saikia, D.J.: Jets in radio galaxies and quasars: an observational perspective. Journal of Astrophysics and Astronomy **43**(2), 97 (2022) https://doi.org/10.1007/s12036-022-09863-2 arXiv:2206.05803 [astro-ph.GA]

[33] Alves, E.P., Zrake, J., Fiuza, F.: Efficient Nonthermal Particle Acceleration by the Kink Instability in Relativistic Jets. Physical Review Letters **121**(24), 245101 (2018) https://doi.org/10.1103/PhysRevLett.121.245101 . Publisher: American Physical Society. Accessed 2024-08-16

[34] Petropoulou, M., Sironi, L., Spitkovsky, A., Giannios, D.: Relativistic Magnetic Reconnection in Electron–Positron–Proton Plasmas: Implications for Jets of Active Galactic Nuclei. The Astrophysical Journal **880**(1), 37 (2019) https://doi.org/10.3847/1538-4357/ab287a . Publisher: The American Astronomical Society. Accessed 2024-08-16

[35] Medina-Torrejón, T.E., Pino, E.M.d.G.D., Kadowaki, L.H.S., Kowal, G., Singh, C.B., Mizuno, Y.: Particle Acceleration by Relativistic Magnetic Reconnection Driven by Kink Instability Turbulence in Poynting Flux–Dominated Jets. The Astrophysical Journal **908**(2), 193 (2021) https://doi.org/10.3847/1538-4357/abd6c2 . Publisher: The American Astronomical Society. Accessed 2024-08-16

[36] Gutiérrez, E.M., Combi, L., Romero, G.E., Campanelli, M.: Non-thermal radiation from dual jet interactions in supermassive black hole binaries. Monthly Notices of the Royal Astronomical Society **532**(1), 506–516 (2024) https://doi.org/10.1093/mnras/stae1473 . Accessed 2024-08-16

[37] Scott, M.A., Readhead, A.C.S.: The low-frequency structure of powerful radio

sources and limits to departures from equipartition. Monthly Notices of the Royal Astronomical Society **180**, 539–550 (1977) https://doi.org/10.1093/mnras/180.4.539 . Publisher: OUP ADS Bibcode: 1977MNRAS.180..539S. Accessed 2024-10-17

[38] Chevalier, R.A.: Synchrotron Self-Absorption in Radio Supernovae. The Astrophysical Journal **499**(2), 810 (1998) https://doi.org/10.1086/305676 . Publisher: IOP Publishing. Accessed 2024-05-01

[39] Panaitescu, A., Kumar, P.: Properties of Relativistic Jets in Gamma-Ray Burst Afterglows. The Astrophysical Journal **571**(2), 779 (2002) https://doi.org/10.1086/340094 . Publisher: IOP Publishing. Accessed 2024-10-17

[40] Rybicki, G.B., Lightman, A.P.: Radiative Processes in Astrophysics. A Wiley-Interscience publication. Wiley, ??? (1991). https://books.google.com/books?id=LtdEjNABMlsC

[41] Tsouros, A., Kylafis, N.D.: The energy distribution of electrons in radio jets. Astronomy & Astrophysics **603**, 4 (2017) https://doi.org/10.1051/0004-6361/201730749 . Publisher: EDP Sciences. Accessed 2024-07-01

[42] Greene, T.P., Kelly, D.M., Stansberry, J., Leisenring, J., Egami, E., Schlawin, E., Chu, L., Hodapp, K.W., Rieke, M.: $\lambda = 2.4$ to 5 μm spectroscopy with the James Webb Space Telescope NIRCam instrument. Journal of Astronomical Telescopes, Instruments, and Systems **3**, 035001 (2017) https://doi.org/10.1117/1.JATIS.3.3.035001 . ADS Bibcode: 2017JATIS...3c5001G. Accessed 2024-09-03

[43] Ivezić, Z., Kahn, S.M., Tyson, J.A., Abel, B., Acosta, E., Allsman, R., Alonso, D., AlSayyad, Y., Anderson, S.F., Andrew, J., Angel, J.R.P., Angeli, G.Z., Ansari, R., Antilogus, P., Araujo, C., Armstrong, R., Arndt, K.T., Astier, P., Aubourg, E., Auza, N., Axelrod, T.S., Bard, D.J., Barr, J.D., Barrau, A., Bartlett, J.G., Bauer, A.E., Bauman, B.J., Baumont, S., Bechtol, E., Bechtol, K., Becker, A.C., Becla, J., Beldica, C., Bellavia, S., Bianco, F.B., Biswas, R., Blanc, G., Blazek, J., Blandford, R.D., Bloom, J.S., Bogart, J., Bond, T.W., Booth, M.T., Borgland, A.W., Borne, K., Bosch, J.F., Boutigny, D., Brackett, C.A., Bradshaw, A., Brandt, W.N., Brown, M.E., Bullock, J.S., Burchat, P., Burke, D.L., Cagnoli, G., Calabrese, D., Callahan, S., Callen, A.L., Carlin, J.L., Carlson, E.L., Chandrasekharan, S., Charles-Emerson, G., Chesley, S., Cheu, E.C., Chiang, H.-F., Chiang, J., Chirino, C., Chow, D., Ciardi, D.R., Claver, C.F., Cohen-Tanugi, J., Cockrum, J.J., Coles, R., Connolly, A.J., Cook, K.H., Cooray, A., Covey, K.R., Cribbs, C., Cui, W., Cutri, R., Daly, P.N., Daniel, S.F., Daruich, F., Daubard, G., Daues, G., Dawson, W., Delgado, F., Dellapenna, A., Peyster, R., Val-Borro, M., Digel, S.W., Doherty, P., Dubois, R., Dubois-Felsmann, G.P., Durech, J., Economou, F., Eifler, T., Eracleous, M., Emmons, B.L., Fausti Neto, A., Ferguson, H., Figueroa, E., Fisher-Levine, M., Focke, W., Foss, M.D., Frank, J., Freemon, M.D., Gangler, E., Gawiser, E., Geary, J.C., Gee, P., Geha, M., Gessner, C.J.B.,

Gibson, R.R., Gilmore, D.K., Glanzman, T., Glick, W., Goldina, T., Goldstein, D.A., Goodenow, I., Graham, M.L., Gressler, W.J., Gris, P., Guy, L.P., Guyonnet, A., Haller, G., Harris, R., Hascall, P.A., Haupt, J., Hernandez, F., Herrmann, S., Hileman, E., Hoblitt, J., Hodgson, J.A., Hogan, C., Howard, J.D., Huang, D., Huffer, M.E., Ingraham, P., Innes, W.R., Jacoby, S.H., Jain, B., Jammes, F., Jee, M.J., Jenness, T., Jernigan, G., Jevremović, D., Johns, K., Johnson, A.S., Johnson, M.W.G., Jones, R.L., Juramy-Gilles, C., Jurić, M., Kalirai, J.S., Kallivayalil, N.J., Kalmbach, B., Kantor, J.P., Karst, P., Kasliwal, M.M., Kelly, H., Kessler, R., Kinnison, V., Kirkby, D., Knox, L., Kotov, I.V., Krabbendam, V.L., Krughoff, K.S., Kubánek, P., Kuczewski, J., Kulkarni, S., Ku, J., Kurita, N.R., Lage, C.S., Lambert, R., Lange, T., Langton, J.B., Le Guillou, L., Levine, D., Liang, M., Lim, K.-T., Lintott, C.J., Long, K.E., Lopez, M., Lotz, P.J., Lupton, R.H., Lust, N.B., MacArthur, L.A., Mahabal, A., Mandelbaum, R., Markiewicz, T.W., Marsh, D.S., Marshall, P.J., Marshall, S., May, M., McKercher, R., McQueen, M., Meyers, J., Migliore, M., Miller, M., Mills, D.J., Miraval, C., Moeyens, J., Moolekamp, F.E., Monet, D.G., Moniez, M., Monkewitz, S., Montgomery, C., Morrison, C.B., Mueller, F., Muller, G.P., Muñoz Arancibia, F., Neill, D.R., Newbry, S.P., Nief, J.-Y., Nomerotski, A., Nordby, M., O'Connor, P., Oliver, J., Olivier, S.S., Olsen, K., O'Mullane, W., Ortiz, S., Osier, S., Owen, R.E., Pain, R., Palecek, P.E., Parejko, J.K., Parsons, J.B., Pease, N.M., Peterson, J.M., Peterson, J.R., Petravick, D.L., Libby Petrick, M.E., Petry, C.E., Pierfederici, F., Pietrowicz, S., Pike, R., Pinto, P.A., Plante, R., Plate, S., Plutchak, J.P., Price, P.A., Prouza, M., Radeka, V., Rajagopal, J., Rasmussen, A.P., Regnault, N., Reil, K.A., Reiss, D.J., Reuter, M.A., Ridgway, S.T., Riot, V.J., Ritz, S., Robinson, S., Roby, W., Roodman, A., Rosing, W., Roucelle, C., Rumore, M.R., Russo, S., Saha, A., Sassolas, B., Schalk, T.L., Schellart, P., Schindler, R.H., Schmidt, S., Schneider, D.P., Schneider, M.D., Schoening, W., Schumacher, G., Schwamb, M.E., Sebag, J., Selvy, B., Sembroski, G.H., Seppala, L.G., Serio, A., Serrano, E., Shaw, R.A., Shipsey, I., Sick, J., Silvestri, N., Slater, C.T., Smith, J.A., Smith, R.C., Sobhani, S., Soldahl, C., Storrie-Lombardi, L., Stover, E., Strauss, M.A., Street, R.A., Stubbs, C.W., Sullivan, I.S., Sweeney, D., Swinbank, J.D., Szalay, A., Takacs, P., Tether, S.A., Thaler, J.J., Thayer, J.G., Thomas, S., Thornton, A.J., Thukral, V., Tice, J., Trilling, D.E., Turri, M., Van Berg, R., Vanden Berk, D., Vetter, K., Virieux, F., Vucina, T., Wahl, W., Walkowicz, L., Walsh, B., Walter, C.W., Wang, D.L., Wang, S.-Y., Warner, M., Wiecha, O., Willman, B., Winters, S.E., Wittman, D., Wolff, S.C., Wood-Vasey, W.M., Wu, X., Xin, B., Yoachim, P., Zhan, H.: LSST: From Science Drivers to Reference Design and Anticipated Data Products. The Astrophysical Journal **873**, 111 (2019) https://doi.org/10.3847/1538-4357/ab042c . Publisher: IOP ADS Bibcode: 2019ApJ...873..111I. Accessed 2024-09-30

[44] Wright, E.L.: A Cosmology Calculator for the World Wide Web. Publications of the Astronomical Society of the Pacific **118**, 1711–1715 (2006) https://doi.org/10.1086/510102 . Publisher: IOP ADS Bibcode: 2006PASP..118.1711W. Accessed 2024-09-30

[45] Gold, R., Paschalidis, V., Etienne, Z.B., Shapiro, S.L., Pfeiffer, H.P.: Accretion

disks around binary black holes of unequal mass: General relativistic magnetohydrodynamic simulations near decoupling. Phys. Rev. D **89**, 064060 (2014) https://doi.org/10.1103/PhysRevD.89.064060

[46] Boerner, T.J., Deems, S., Furlani, T.R., Knuth, S.L., Towns, J.: ACCESS: Advancing Innovation: NSF's Advanced Cyberinfrastructure Coordination Ecosystem: Services & Support. In: Practice and Experience in Advanced Research Computing 2023: Computing for the Common Good. PEARC '23, pp. 173–176. Association for Computing Machinery, New York, NY, USA (2023). https://doi.org/10.1145/3569951.3597559 . https://dl.acm.org/doi/10.1145/3569951.3597559 Accessed 2024-09-12

[47] Ansorg, M., Brügmann, B., Tichy, W.: Single-domain spectral method for black hole puncture data. Physical Review D **70**, 064011 (2004) https://doi.org/10.1103/PhysRevD.70.064011 . ADS Bibcode: 2004PhRvD..70f4011A. Accessed 2024-03-20

[48] Balbus, S.A., Hawley, J.F.: A powerful local shear instability in weakly magnetized disks. i - linear analysis. ii - nonlinear evolution. The Astrophysical Journal **376**, 214 (1991) https://doi.org/10.1086/170270

[49] Shibata, M., Nakamura, T.: Evolution of three-dimensional gravitational waves: Harmonic slicing case. Phys. Rev. D **52**, 5428–5444 (1995) https://doi.org/10.1103/PhysRevD.52.5428

[50] Baumgarte, T.W., Shapiro, S.L.: Numerical integration of einstein's field equations. Phys. Rev. D **59**, 024007 (1998) https://doi.org/10.1103/PhysRevD.59.024007

[51] Sperhake, U.: Binary black-hole evolutions of excision and puncture data. Physical Review D **76**(10), 104015 (2007) https://doi.org/10.1103/PhysRevD.76.104015 . Publisher: American Physical Society. Accessed 2023-10-20

[52] Baker, J.G., Centrella, J., Choi, D.-I., Koppitz, M., Meter, J.: Gravitational-Wave Extraction from an Inspiraling Configuration of Merging Black Holes. Physical Review Letters **96**(11), 111102 (2006) https://doi.org/10.1103/PhysRevLett.96.111102 . Publisher: American Physical Society. Accessed 2024-09-26

[53] Campanelli, M., Lousto, C.O., Marronetti, P., Zlochower, Y.: Accurate Evolutions of Orbiting Black-Hole Binaries without Excision. Physical Review Letters **96**(11), 111101 (2006) https://doi.org/10.1103/PhysRevLett.96.111101 . Publisher: American Physical Society. Accessed 2024-09-26

[54] Etienne, Z.B., Paschalidis, V., Haas, R., Moesta, P., Shapiro, S.L.: IllinoisGRMHD: An Open-Source, User-Friendly GRMHD Code for Dynamical Spacetimes. Classical and Quantum Gravity **32**(17), 175009 (2015) https://doi.org/10.1088/0264-9381/32/17/175009 . arXiv:1501.07276 [astro-ph, physics:gr-qc].

Accessed 2023-08-04

[55] Werneck, L., Cupp, S., Assumpção, T., Brandt, S.R., Cheng, C.-H., Diener, P., Doherty, J., Etienne, Z., Haas, R., Jacques, T.P., Karakaş, B., Topolski, K., Tsao, B.-J., Alcubierre, M., Alic, D., Allen, G., Ansorg, M., Babiuc-Hamilton, M., Baiotti, L., Benger, W., Bentivegna, E., Bernuzzi, S., Bode, T., Bozzola, G., Brendal, B., Bruegmann, B., Campanelli, M., Cipolletta, F., Corvino, G., Pietri, R.D., Dima, A., Dimmelmeier, H., Dooley, R., Dorband, N., Elley, M., Khamra, Y.E., Faber, J., Ficarra, G., Font, T., Frieben, J., Giacomazzo, B., Goodale, T., Gundlach, C., Hawke, I., Hawley, S., Hinder, I., Huerta, E.A., Husa, S., Ikeda, T., Iyer, S., Ji, L., Johnson, D., Joshi, A.V., Kalyanaraman, H., Kankani, A., Kastaun, W., Kellermann, T., Knapp, A., Koppitz, M., Kuo, N., Laguna, P., Lanferman, G., Lasky, P., Leung, L., Löffler, F., Macpherson, H., Masso, J., Menger, L., Merzky, A., Miller, J.M., Miller, M., Moesta, P., Montero, P., Mundim, B., Nelson, P., Nerozzi, A., Noble, S.C., Ott, C., Papenfort, L.J., Paruchuri, R., Pollney, D., Price, D., Radice, D., Radke, T., Reisswig, C., Rezzolla, L., Richards, C.B., Rideout, D., Ripeanu, M., Sala, L., Schewtschenko, J.A., Schnetter, E., Schutz, B., Seidel, E., Seidel, E., Shalf, J., Sible, K., Sperhake, U., Stergioulas, N., Suen, W.-M., Szilagyi, B., Takahashi, R., Thomas, M., Thornburg, J., Tian, C., Tobias, M., Tonita, A., Tootle, S., Walker, P., Wan, M.-B., Wardell, B., Wen, A., Witek, H., Zilhão, M., Zink, B., Zlochower, Y.: The Einstein Toolkit. Zenodo. To find out more, visit http://einsteintoolkit.org (2023). https://doi.org/10.5281/zenodo.7942541 . https://doi.org/10.5281/zenodo.7942541

[56] Schnetter, E., Hawley, S., Hawke, I.: Carpet: Adaptive Mesh Refinement for the Cactus Framework. Astrophysics Source Code Library, 1611–016 (2016). ADS Bibcode: 2016ascl.soft11016S. Accessed 2024-09-03

[57] Toro, E.F.: Riemann Solvers and Numerical Methods for Fluid Dynamics: A Practical Introduction. Springer, Berlin, Heidelberg (2009). https://doi.org/10.1007/b79761 . https://link.springer.com/10.1007/b79761 Accessed 2024-09-13

[58] Colella, P., Woodward, P.R.: The Piecewise Parabolic Method (PPM) for gas-dynamical simulations. Journal of Computational Physics **54**(1), 174–201 (1984) https://doi.org/10.1016/0021-9991(84)90143-8 . Accessed 2024-09-13

[59] Porth, O., Chatterjee, K., Narayan, R., Gammie, C.F., Mizuno, Y., Anninos, P., Baker, J.G., Bugli, M., Chan, C.-k., Davelaar, J., Del Zanna, L., Etienne, Z.B., Fragile, P.C., Kelly, B.J., Liska, M., Markoff, S., McKinney, J.C., Mishra, B., Noble, S.C., Olivares, H., Prather, B., Rezzolla, L., Ryan, B.R., Stone, J.M., Tomei, N., White, C.J., Younsi, Z., Akiyama, K., Alberdi, A., Alef, W., Asada, K., Azulay, R., Baczko, A.-K., Ball, D., Baloković, M., Barrett, J., Bintley, D., Blackburn, L., Boland, W., Bouman, K.L., Bower, G.C., Bremer, M., Brinkerink, C.D., Brissenden, R., Britzen, S., Broderick, A.E., Broguiere, D., Bronzwaer, T., Byun, D.-Y., Carlstrom, J.E., Chael, A., Chatterjee, S., Chen, M.-T., Chen, Y., Cho, I.,

Christian, P., Conway, J.E., Cordes, J.M., Geoffrey, Crew, B., Cui, Y., De Laurentis, M., Deane, R., Dempsey, J., Desvignes, G., Doeleman, S.S., Eatough, R.P., Falcke, H., Fish, V.L., Fomalont, E., Fraga-Encinas, R., Freeman, B., Friberg, P., Fromm, C.M., Gómez, J.L., Galison, P., García, R., Gentaz, O., Georgiev, B., Goddi, C., Gold, R., Gu, M., Gurwell, M., Hada, K., Hecht, M.H., Hesper, R., Ho, L.C., Ho, P., Honma, M., Huang, C.-W.L., Huang, L., Hughes, D.H., Ikeda, S., Inoue, M., Issaoun, S., James, D.J., Jannuzi, B.T., Janssen, M., Jeter, B., Jiang, W., Johnson, M.D., Jorstad, S., Jung, T., Karami, M., Karuppusamy, R., Kawashima, T., Keating, G.K., Kettenis, M., Kim, J.-Y., Kim, J., Kim, J., Kino, M., Koay, J.Y., Patrick, Koch, M., Koyama, S., Kramer, M., Kramer, C., Krichbaum, T.P., Kuo, C.-Y., Lauer, T.R., Lee, S.-S., Li, Y.-R., Li, Z., Lindqvist, M., Liu, K., Liuzzo, E., Lo, W.-P., Lobanov, A.P., Loinard, L., Lonsdale, C., Lu, R.-S., MacDonald, N.R., Mao, J., Marrone, D.P., Marscher, A.P., Martí-Vidal, I., Matsushita, S., Matthews, L.D., Medeiros, L., Menten, K.M., Mizuno, I., Moran, J.M., Moriyama, K., Moscibrodzka, M., Müller, C., Nagai, H., Nagar, N.M., Nakamura, M., Narayanan, G., Natarajan, I., Neri, R., Ni, C., Noutsos, A., Okino, H., Oyama, T., Özel, F., Palumbo, D.C.M., Patel, N., Pen, U.-L., Pesce, D.W., Piétu, V., Plambeck, R., PopStefanija, A., Preciado-López, J.A., Psaltis, D., Pu, H.-Y., Ramakrishnan, V., Rao, R., Rawlings, M.G., Raymond, A.W., Ripperda, B., Roelofs, F., Rogers, A., Ros, E., Rose, M., Roshanineshat, A., Rottmann, H., Roy, A.L., Ruszczyk, C., Rygl, K.L.J., Sánchez, S., Sánchez-Arguelles, D., Sasada, M., Savolainen, T., Schloerb, F.P., Schuster, K.-F., Shao, L., Shen, Z., Small, D., Sohn, B.W., SooHoo, J., Tazaki, F., Tiede, P., Tilanus, R.P.J., Titus, M., Toma, K., Torne, P., Trent, T., Trippe, S., Tsuda, S., Bemmel, I., Langevelde, H.J., Rossum, D.R., Wagner, J., Wardle, J., Weintroub, J., Wex, N., Wharton, R., Wielgus, M., Wong, G.N., Wu, Q., Young, K., Young, A., Yuan, F., Yuan, Y.-F., Zensus, J.A., Zhao, G., Zhao, S.-S., Zhu, Z., Event Horizon Telescope Collaboration: The Event Horizon General Relativistic Magnetohydrodynamic Code Comparison Project. The Astrophysical Journal Supplement Series **243**, 26 (2019) https://doi.org/10.3847/1538-4365/ab29fd . ADS Bibcode: 2019ApJS..243...26P. Accessed 2024-03-20

[60] Farris, B.D., Gold, R., Paschalidis, V., Etienne, Z.B., Shapiro, S.L.: Binary Black-Hole Mergers in Magnetized Disks: Simulations in Full General Relativity. Physical Review Letters **109**(22), 221102 (2012) https://doi.org/10.1103/PhysRevLett.109.221102 . Publisher: American Physical Society. Accessed 2024-09-28

[61] Thornburg, J.: A fast apparent horizon finder for three-dimensional Cartesian grids in numerical relativity. Class. & Quant. Gravity **21**, 743–766 (2004) https://doi.org/10.1088/0264-9381/21/2/026 gr-qc/0306056

[62] Virtanen, P., Gommers, R., Oliphant, T.E., Haberland, M., Reddy, T., Cournapeau, D., Burovski, E., Peterson, P., Weckesser, W., Bright, J., van der Walt, S.J., Brett, M., Wilson, J., Millman, K.J., Mayorov, N., Nelson, A.R.J., Jones,

E., Kern, R., Larson, E., Carey, C.J., Polat, İ., Feng, Y., Moore, E.W., VanderPlas, J., Laxalde, D., Perktold, J., Cimrman, R., Henriksen, I., Quintero, E.A., Harris, C.R., Archibald, A.M., Ribeiro, A.H., Pedregosa, F., van Mulbregt, P., SciPy 1.0 Contributors: SciPy 1.0: Fundamental Algorithms for Scientific Computing in Python. Nature Methods **17**, 261–272 (2020) https://doi.org/10.1038/s41592-019-0686-2

[63] Witek, H., Zilhao, M., Bozzola, G., Elley, M., Ficarra, G., Ikeda, T., Sanchis-Gual, N., Silva, H.: Canuda: a Public Numerical Relativity Library to Probe Fundamental Physics. https://doi.org/10.5281/zenodo.5520862 . https://doi.org/10.5281/zenodo.5520862

[64] Bozzola, G.: kuibit: Analyzing Einstein Toolkit simulations with Python. The Journal of Open Source Software **6**(60), 3099 (2021) https://doi.org/10.21105/joss.03099 arXiv:2104.06376 [gr-qc]